

# **Removal of Boron from Aqueous Solutions by Adsorption Using Fly Ash, Zeolite and Demineralized Lignite**

**Seren Yüksel and Yuda Yürüm\***

Faculty of Engineering and Natural Sciences  
Sabanci University  
Orhanli, Tuzla, Istanbul 34956, Turkey  
[yyurum@sabanciuniv.edu](mailto:yyurum@sabanciuniv.edu)

\*Corresponding author.

Yuda Yürüm

Faculty of Engineering and Natural Sciences  
Sabanci University

Orhanli, Tuzla, Istanbul 34956, Turkey

Phone: 90 216 4839512, Fax: 90 216 4839550

[yyurum@sabanciuniv.edu](mailto:yyurum@sabanciuniv.edu)

# Removal of Boron from Aqueous Solutions by Adsorption Using Fly Ash, Zeolite and Demineralized Lignite

**Seren Yüksel and Yuda Yürüm\***

Faculty of Engineering and Natural Sciences

Sabanci University

Orhanli, Tuzla, Istanbul 34956, Turkey

[yyurum@sabanciuniv.edu](mailto:yyurum@sabanciuniv.edu)

**Abstract:** In the present study for the purpose of removal of boron from water by adsorption using adsorbents like fly ash, natural zeolite and demineralized lignite was investigated. Boron in water was removed with fly ash, zeolite and demineralized lignite with different capacities. 94% boron was removed using fly ash. Batch experiments were conducted to test removal capacity, to obtain adsorption isotherms, thermodynamic and kinetic parameters. Boron removal by all adsorbents was affected by pH of solution; maximum adsorption was achieved at pH 10. Adsorption of boron on fly ash was investigated by Langmuir, Freundlich, Dubinin-Radushkevich models. Standard entropy and enthalpy changes of adsorption of boron on fly ash were,  $\Delta S^0 = -0.69$  kJ/mol K and  $\Delta H^0 = -215.34$  kJ/mol, respectively. The negative value of  $\Delta S^0$  indicated decreased randomness at the solid/solution interface during the adsorption boron on the fly ash sample. Negative values of  $\Delta H^0$  showed the exothermic nature of the process. The negative values of  $\Delta G^0$  implied that the adsorption of boron on fly ash samples was spontaneous. Adsorption of boron on fly ash occurred with a pseudo-second order kinetic model, intraparticle diffusion of boron species had also some effect in adsorption kinetics.

**Keywords:** Boron, boric acid, borate ion, fly ash, coal, zeolite, adsorption, Langmuir isotherm, Freundlich isotherm, Dubinin-Radushkevich model.

## INTRODUCTION

The U.S. Bureau of Mines and U.S. Geological Survey, report that world production of borate minerals and boron chemical derivatives are about  $5 \times 10^6$  tons of  $B_2O_3$  per year and world reserves are calculated as  $270 \times 10^6$  tons (in  $B_2O_3$  form). The United States (42%), Turkey (42%) and South America (11%) are the biggest producers and they constitute about 95% of borate production worldwide [1]. The occurrence of boron compounds in waters increases in a continuous and parallel way to industrial development. The main boron sources, whose presence is detected in surface waters, are urban wastes rich in detergents and cleaning products; industrial wastes, which can come from a wide range of different activities as well as several chemical products used in agriculture [2]. Boron is generally found in natural water as boric acid,  $B(OH)_3$ , and/or borate ion,  $B(OH)_4^-$  [3].

Boron is an essential nutrient for plants, but can be toxic to organisms when accumulated in high concentrations. Boron is widely distributed in nature in low concentrations, and is usually  $<0.1\text{--}0.5$  ppm in surface freshwaters; but its higher concentrations are measured in a few areas [3,4]. High levels of boron concentrations in the range of 1-63 ppm causes environmental problems in ground thermal waters and surface waters in some agricultural areas of western Anatolia. Sericite, illite and tourmaline minerals, which are abundant in Menderes Massif rocks, are considered to be the main reason for the high boron contents [5]. Kizildere, which is the only commercial geothermal power plant in Turkey and located in Büyük Menderes river in south-west Turkey, discharges annually 6 million tons of wastewater into the Büyük Menderes river, creating environmental pollution. Currently, the wastewater, which includes up to 24 ppm boron, is discharged into the river at a rate of 750–1500 tons per hour [6]. Boron concentrations of 4.7 ppm in seawater, 0.5-2 ppm in domestic wastewater and up to 8 ppm in regional groundwater are measured in Italy, Cyprus and Greece. According to Demirel and Yildirim [7], the World Health Organization defined boron level of 0.3 ppm as the non-observed effect level for drinking water. In 1998 the European Union (EU) revised its Drinking Water Directive, which is responsible for regulating the quality of water in the EU intended for human consumption. Specifically, the EU added a new standard for boron in drinking water (1 ppm) and countries such as Italy and Cyprus with high natural boron concentrations in their drinking water are, thus, finding that compliance with the new EU boron regulation is more difficult and expensive than originally

anticipated [8]. High boron levels in drinking water can be toxic to humans as boron has been shown to cause male reproductive obstructions in laboratory animals [9-11].

Standard wastewater treatment methods and desalination of seawater by reverse osmosis are not successfully employed for the elimination of boron from raw waters [12]. Owing to the majority of the non-charged boric acid in the solution, only a fraction of the boron is removed during reverse osmosis desalination [13-18]. Seawater contains approximately 5 ppm of boron. In most cases, the rejection of boron by reverse osmosis is not sufficiently high, so about one third of boron content (~1.5 ppm) is normally found in permeate [19]. The ion-exchange resin Amberlite IRA-743 is boron specific and has the capacity of almost to remove 100% of boron under high pH conditions [20-21] and has been previously used to remove boron from raw waters in Turkey [22-24].

Removing boric acid and borate ions from aqueous solutions does not seem to be straightforward, as has already been stated in the literature [25]. Conventional sedimentation and biological treatment remove insignificant amounts of boron from waters. Chemicals normally used in the water treatment industry do not have any effect on the boron levels in water. The adsorption of boron by clays, soils and other minerals has been extensively studied by many investigators [26-35]. Polat et al. [36] conducted various column and batch experiments that explored the efficiency of boron removal from seawater and desalinated seawater using several types of coal and fly ash materials under controlled conditions (pH, liquid/solid ratio, time of reaction, pre-treatment, regeneration) and reported that their experiments showed a considerable amount of boron (>90%) can be removed due to interaction with fly ash and coal under suitable conditions of high pH (>9), low liquid/solid ratio (<20), and reaction time (>6 h). A recent preliminary study [37] showed that activated alumina could be also a suitable adsorbent for the removal of boron from water. The adsorption was strongly dependent on pH, adsorbent dose and boron concentration. For initial concentration of 5 and 50 ppm, the maximum uptake of boron reaches respectively 40% and 65% for an adsorbent dose of 0.8 and 5 g.

In the present report, removal of boron from water by adsorption using adsorbents like fly ash, natural zeolite and demineralized lignite was investigated for the purpose of treatment of fresh water polluted with boron.

## **EXPERIMENTAL**

### **Materials**

The fly ash was obtained from Kemerköy thermal power plant, Milas, Mugla, Turkey. The fly ash had basic pH values that changed in the range of 11-12. The main component of the fly ash is CaO (44.2 %) and CaO was the component that gave this basic property to the fly ash. Turkish Gördes-Kalabak zeolite sample was used in the present study. The type of mineral in zeolite was clinoptilolite. The clinoptilolite content of the zeolite was 95% (by weight). The clinoptilolite of the sample is K and Ca rich type. The chemical analyses and surface characteristics of adsorbents are given in Table 1.

Demineralized Turkish Beypazari lignite was used as an adsorbent in the present study (Table 1). Because the boron content in raw lignite was 291 ppm also [38]. Therefore Beypazari lignite was demineralized according to standard methods described previously [39]. In the first step, coal samples were treated with 5 % HCl solution at 60°C for 1 hour while being stirred. During this treatment, 250 ml of solution was used for each 40 g coal. After 1 hour, the coal was filtered, washed with distilled water and dried in an oven. Second step was HF treatment, in which 200 ml of concentrated HF was used for each 30 g of sample. The coal was placed in a concentrated HF solution and kept at room temperature without stirring for 1 hour. In this step, no glassware but polypropylene laboratory ware was used. After the samples were filtered, washed with distilled water and dried, the third treatment was performed. This involved placing the coal in concentrated HCl at room temperature for 1 hour without stirring. After filtration, washing and drying the lignite, the demineralization was completed. Demineralized lignite was analyzed for boron using inductively coupled plasma (ICP) spectrophotometer and B<sub>2</sub>O<sub>3</sub> was not detected in this sample (Table 1).

### **Adsorption Experiments**

A series of batch adsorption tests are conducted to evaluate the effects of certain parameters, such as pH, initial boron concentration, adsorbent dose and time. The adsorbents used were fly ash, natural zeolite and demineralized lignite. All adsorbents were dried for 2 hours before adsorption experiments. To investigate the effect of pH of the boric acid solutions a set of samples were prepared. The pH of these boric acid solutions, of 10 ppm (~1 mmol/L) B

concentration was adjusted to values between 2 and 11 using 1M HNO<sub>3</sub> or 1M NaOH solutions. The pH of the solutions was kept constant during the adsorption process in all of the experiments. Samples of 50 mL of volume of these solutions were mixed with 2 g of adsorbent and shaken in an incubator shaker at 150 rpm mixing rate for 24 hours. At the end of experiment the solution was separated from the solid adsorbent by filtration and the filtrate was analyzed for boron concentration using inductively coupled plasma (ICP) spectrophotometry.

After setting the best pH value (pH=10), to determine the optimum adsorbent dose, adsorption experiments with increasing amounts of adsorbents (20-200 g/L) were conducted. 50 mL of boric acid solutions, of 10 ppm (~1 mmol/L) B concentration were shaken at 150 rpm mixing rate with adjusted amounts of adsorbents for 24 hours. Again at the end of experiment the solution was separated from the solid adsorbent by filtration and the filtrate was analyzed for boron concentration using ICP spectrophotometry.

To determine the time required to reach steady state in adsorption, solutions of 50 ml with 10 ppm (~1 mmol/L) B concentration, with optimum pH and using the optimum adsorbent dose were shaken for time intervals changing from 1 to 30 hours. At the end of each experiment the amount of boron adsorbed determined.

After setting the optimum pH, adsorbent dose and time to reach steady state, adsorption isotherms were determined at different temperatures. Adsorption of different initial boron concentrations was examined under optimum conditions determined previously. Boric acid solutions with boron concentrations between 5 ppm (~0.5 mmol/L) and 20 ppm (~2 mmol/L) were prepared and shaken with adsorbents for 24 hours. Experiments were performed for all of the adsorbents at 25°C and 150 rpm mixing rate. Since maximum adsorption was observed with fly ash, additional experiments were made using fly ash as adsorbent at 35°C and 45°C. After each experiment, adsorption of boron was analyzed with ICP spectrophotometry. Each adsorption experiment in the present study in order to have average values was at least repeated 5 times before they were reported below.

## **Analytical Techniques**

### Chemical analyses of adsorbents

Chemical analysis results of the adsorbents used, reported within the text and in Table 1 are those obtained from the suppliers of these materials. General elemental analyses techniques for the lignite and wet chemical analyses techniques for zeolite and fly ash were used in the analyses of these materials.

### Boron concentration

Boron concentrations of the solutions were measured with a Varian, Vista-Pro CCD simultaneous inductively coupled plasma ICP-OES spectrophotometer. Samples before and after adsorption experiments were analyzed for boron.

### Scanning electron microscopy (SEM)

Leo Supra 35VP Field emission scanning electron microscope, Leo 32 and electron dispersive spectrometer software was used for images and analysis. Imaging was generally done at 2-5 keV accelerating voltage, using the secondary electron imaging technique.

### XRD measurements

XRD measurements of the carbonized and activated product samples were done with a Bruker axis advance powder diffractometer fitted with a Siemens X-ray gun and equipped with Bruker axis Diffrac PLUS software. The sample was rotated (20 rpm) and swept from  $2\theta = 5^\circ$  through to  $80^\circ$  using default parameters of the program. The X-ray generator was set to 40kV at 40 mA. All the XRD measurements were repeated at least three times and the results reported were the average of these measurements.

## Surface analyses

Surface area and pore analyses were performed with a NOVA 2200e Surface Area and Pore Size analyzer.

### Adsorption Isotherms

Langmuir and Freundlich isotherms were checked for the adsorption of boron on the adsorbents used in the present study. Langmuir equation was employed to obtain monolayer capacity and is represented as,

$$C_e / C_s = 1 / (C_m \mathcal{L}) + C_e / C_m \quad (1)$$

where  $C_s$  is the amount adsorbed on solid (mmol/g),  $C_e$  is the equilibrium solution concentration (mmol/L),  $C_m$  is adsorption capacity (maximum amount that can be adsorbed by adsorbent as monolayer (mmol/g), and  $\mathcal{L}$  is a constant related to adsorption energy (L/mmol) [40].

Freundlich isotherm is not limited to the creation of the monolayer coverage and it supposes that adsorption happens on heterogeneous surface of solid. Freundlich equation was utilized to measure relative adsorption capacity and the relation can be given as,

$$C_s = K_f C_e^{n_f} \quad (2)$$

where  $C_s$ , is the amount of adsorbed of solute (mmol/g);  $C_e$ , equilibrium solution concentration of solute (mmol/L);  $K_f$ , (mmol/g) can be considered as a measurement of the relative adsorption capacity since it is the value of  $C_s$ , when  $C_e$  is unity.  $n_f$  is a constant related to the adsorption intensity of the adsorbent. The Freundlich equation can be linearized by taking logarithms of the equation,

$$\ln C_s = \ln K_f + n_f \ln C_e \quad (3)$$

$K_f$  and  $n_f$  values were obtained by plotting  $\ln C_s$  versus  $\ln C_e$ . The isotherm parameters were determined by nonlinear regression through the linearized form of Freundlich equation (3).

It is known that Langmuir and Freundlich isotherms could not show the adsorption mechanism. In order to explain the adsorption type, equilibrium data was applied to Dubinin–Radushkevich (DR) isotherm with the equation

$$\ln C_s = \ln X_m - k \varepsilon^2 \quad (4)$$

where  $\varepsilon$  is Polanyi potential, equal to  $RT \ln (1 + 1/C_e)$ ,  $C_s$  is the amount of adsorbate adsorbed per unit weight of adsorbent (mol/g),  $C_e$  is the equilibrium concentration of boron (mol/L),  $X_m$

is the adsorption capacity (mol/g),  $k$  is a constant related to adsorption energy ( $\text{mol}^2/\text{kJ}^2$ ),  $T$  is the temperature (K), and  $R$  is the gas constant ( $\text{kJ}/\text{molK}$ ).  $X_m$  and  $k$  values were obtained by plotting  $\ln C_s$  versus  $\varepsilon^2$  at various temperatures. The slope of line yields  $k$  ( $\text{mol}^2/\text{kJ}^2$ ) and the intercept is equal to  $\ln X_m$  [41]. These calculations were done on the assumption that the application condition of the DR isotherm depended on monolayer adsorption or heterogenous adsorption.

The mean free energy of adsorption (the free energy change one mol adsorbate in transferred from infinity in solution to the surface of the adsorbent) was obtained from the following relationship [41],

$$E = -(2k)^{-0.5} \quad (6)$$

If  $E$  is less than 8 kJ/mol, it can be said that the adsorption is physical adsorption due to weak van der Waals forces [42,43].

### Thermodynamics of Adsorption

In order to understand the effect of temperature on the adsorption process, thermodynamic parameters should be determined at various temperatures. The molar free energy change of the adsorption process is related to the equilibrium constant ( $K_c$ ) and calculated from the equation:

$$\Delta G^\circ = -RT \ln K_c \quad (7)$$

where  $R$  is the gas constant ( $8.314 \text{ J}/\text{molK}$ ),  $T$  is the absolute temperature.  $K_c$  (L/g) values were estimated as:

$$K_c = C_s/C_e \quad (8)$$

where  $C_s$  is the equilibrium concentration of boron on adsorbent (mmol/g),  $C_e$  is the equilibrium concentration of boron in the solution (mmol/L). Each  $K_c$  value was the average of all experimental values ( $C_s/C_e$ ) obtained at constant temperature that the adsorption experiments were done.

Standard enthalpy change,  $\Delta H^\circ$ , and standard entropy change,  $\Delta S^\circ$ , of adsorption can be estimated using the following equation:

$$\ln K_c = -\Delta H^\circ_{ads}/RT + \Delta S^\circ_{ads}/R \quad (9)$$

Looking at the equation (9) above, a plot of  $\ln K_c$  against  $1/T$  renders a straight line. The slope of that straight line is equal to  $-\Delta H^o_{ads}/R$  and its intercept value is equal to  $\Delta S^o_{ads}/R$ .

### Kinetics of Adsorption

The pseudo-first order equation, the pseudo-second-order equation, and the intraparticle diffusion model were employed with the equations [44-46].

$$1/q_t = (k_1/q_1)(1/t) + 1/q_1 \quad (10)$$

$$t/q_t = (1/k_2q_2^2) + t/q_2 \quad (11)$$

$$q_t = k_p t^{1/2} + C \quad (12)$$

Where,  $q_t$  is the amount of boron adsorbed (mg/g) at time  $t$ ,  $q_1$  is the maximum adsorption capacity (mg/g) for pseudo first-order adsorption,  $k_1$  is the pseudo-first-order rate constant for the boron adsorption process ( $\text{hr}^{-1}$ ),  $q_2$  is the maximum adsorption capacity for the pseudo second order adsorption (g/mg hr),  $k_2$  is the pseudo second order rate constant ( $\text{hr}^{-1}$ ),  $k_p$  is the intraparticle diffusion rate constant ( $\text{mg/g hr}^{1/2}$ ), and  $C$  is the intercept.

## RESULTS AND DISCUSSION

### Characterization of Adsorbents

In addition to chemical analyses, the surface areas of the adsorbents and their pore radii are also given in Table 1. Although the surface area of demineralized lignite ( $31.1 \text{ m}^2/\text{g}$ ) and zeolite ( $10.2 \text{ m}^2/\text{g}$ ) seemed to be greater than that of fly ash ( $7.2 \text{ m}^2/\text{g}$ ), percentage of boron separated using fly ash was greater than the percentages of boron separated using demineralized lignite and zeolite in every comparable experiment. Pore radius of the fly ash ( $57.5 \text{ nm}$ ) used was much greater than those of zeolite ( $22.1 \text{ nm}$ ) and demineralized lignite ( $23.7 \text{ nm}$ ). This might be an important reason of enhanced adsorption of boron on fly ash compared to other adsorbents. Another reason for the adsorption of boron species on to the fly ash might be the high CaO content of the fly ash. CaO might have chemically reacted with boron species and thus removal of boron might have thus increased to higher values than those observed with demineralized lignite and zeolite.

SEM images of fly ash, demineralized lignite and zeolite are presented in Fig.1. The SEM of fly ash (Fig. 1 a) shows a heterogeneous material consisting largely of small spheres, formed by the condensation of aluminous and siliceous glass droplets in the air. Also found in

fly ash sample are irregular, porous, coke-like particles of unburned carbon material, which are often concentrated in the larger size fractions. Fig. 1a clearly shows that finer fly ash particles (about 1  $\mu\text{m}$ ) are primarily spherical, whereas the coarser particles are mainly composed of irregular and porous particles. SEM micrograph of the residual coal leached with acid mixture is displayed in Fig. 1b. Some disintegration of the organic part of the coal after acid treatment can be seen. Fig. 1c shows the SEM image of the zeolite sample. The natural zeolite sample which contained porous structure demonstrated some heterogeneously distributed network comprised of small fistulous and filamentous crystallites.

The crystalline phases of fly ash were determined by XRD analyses. Fig. 2 shows the XRD patterns of fly ash. The results indicate that the fly ash is composed of quartz, kaolinite and calcium oxide. The X-ray diffractogram of the zeolite is shown in Fig. 3. The powder XRD pattern of the zeolite is characterized by many peaks due its structure ordering. The XRD pattern shows sharp and symmetric peaks, which are characteristic of lamellar compounds, and also indicate a high degree of crystallinity of the zeolite sample. XRD patterns for demineralized lignite along with the one for raw lignite for comparison are shown in Fig. 4. Hydrochloric acid treatment dissolved carbonate minerals of the lignite and hydrofluoric acid was used to dissolve the silicate minerals. In the diffractogram of the demineralized lignite peaks attributed to carbonate and silicate minerals are absent. The XRD pattern for demineralized lignite is a continuous line corresponding to amorphous carbon, while distinct peaks found in raw lignite and referring to different mineral species have disappeared. Peaks related to inorganic minerals of kaolinite, calcite, quartz and pyrite [47] are shown in the diffractogram of the raw lignite, Fig. 4a.

### **Effect of pH on Adsorption of Boron**

The efficiency of using fly ash, coal and zeolite for boron removal from aqueous solutions was tested with several operational parameters such as pH, time of reaction, material type, amount of adsorbent (g of adsorbent/L of solution). The pH controls the adsorption at the water adsorbent interfaces. The pH value of the solution was an important controlling parameter in the adsorption process. The form of boron in solution depends strongly on the pH and takes the forms of  $\text{B}(\text{OH})_3$  at low pHs or  $\text{B}(\text{OH})_4^-$  at high pHs. Hence, optimization of pH for adsorption of boron was done by studying the uptake of boron over fly ash, demineralized lignite and zeolite as a function of pH. The pH value of the solution was an

important controlling parameter in the adsorption process. Adsorption of boron as a function of pH for fly ash, demineralized lignite and zeolite at 25°C, with an adsorbent concentration of 40 g/L and an initial boron concentration of about 10 ppm (~1 mmol/L) and adsorption time of 24 hours is presented in Fig. 5. The dependence of the adsorption of boron on the pH of the solution has been studied to achieve the optimum pH value and a better understanding of the adsorption mechanism. The results showed that boron removal by all adsorbents depended on the pH of the solution [36]. It has been found that maximum adsorption of boron from aqueous solutions takes place at pH range of 10-11. Decreased adsorption values were observed at lower pH values. Therefore, all adsorption experiments were conducted at pH 10. The amount of boron removed was higher in the case of fly ash. When the pH was in the range of 10-11, boron removal by fly ash increased to about 94 %. Demineralized lignite and zeolite seemed to be not very effective compared to fly ash. Boron removal by demineralized coal and zeolite reached to maximum values of about 18 % at the same pH values.

### **Effect of Amount of Adsorbent on Boron Sorption**

It is essential to determine the optimum amount of adsorbent, (g adsorbent/L of solution), in order to avoid an excessive consumption of the adsorbent, which makes the process more complicated without achieving a significant increase in the removal yield. The amounts of adsorbent studied and their corresponding amounts of boron removal, stated as percentages, are shown in Fig. 6. The amount of boron removed from aqueous boron solutions increased by increasing the adsorbent quantity for all the adsorbents. It can be observed that the process is strongly influenced in the beginning by the quantity of adsorbent present. A significant positive slope is revealed. Adsorption of boron with the amount of adsorbent increased in all of the adsorbents. The effect was more pronounced in the case of fly ash. As the amount of the fly ash was increased from 20 g/L to 100.0 g/L, the percentage of adsorbed boron increased from 47 to 94, respectively. Further increase in the amount of the fly ash did not change the percentage of the adsorbed boron significantly. The situation in the case of demineralized lignite and zeolite was similar, but the boron adsorbed remained at much lower values of 16.9 % and 15.8 %, respectively, when the amount of the adsorbents was increased from 20 g/L to 50 g/L. Increasing the amount of demineralized lignite and zeolite up to 200 g/L changed the percentage of adsorbed boron only to 17.3% and 15.4%, respectively.

Therefore the optimum values of the amount of adsorbents was found to be for fly ash, demineralized lignite and zeolite, 100 g/L, 50 g/L and 50 g/L, respectively.

### Adsorption Isotherms

The sorption experiments of boron were performed in the batch mode. The equilibrium relationship between the amount of boron adsorbed per unit mass of the sorbent and the residual boron concentration in solution phase were expressed by adsorption isotherms.

The adsorption isotherms of boron in aqueous solution for fly ash at different temperatures are shown in Fig. 7 and those of demineralized lignite and zeolite at 25 °C are shown in Figure 8. As can be seen from the curves, it can be concluded that the amount of adsorbed boron increased as its equilibrium concentration in solution increased. The isotherms for all adsorbents can be classified as type I isotherm. In the type I case, the amount adsorbed component increases steadily with concentration until a plateau is reached where surface of the adsorbent practically is saturated. No further adsorption occurs at this stage. This isotherm describes 'ideal' chemisorption, where molecules chemisorb until the surface becomes saturated with adsorbate, whereupon adsorption ceases. Type I behavior is generally explained with Langmuir isotherm.

The applicability of the Langmuir and Freundlich sorption isotherms were tested under these specified conditions. The data obtained from the adsorption process was fitted into the linearly transformed Langmuir and Freundlich adsorption isotherms. The values of Langmuir and Freundlich isothermal constants, obtained from the linear fits of the data obtained at 25°C are presented in Table 2. The data obtained in the present work nicely fit the Langmuir and Freundlich models. Analyses of the results obtained revealed that the adsorption of boron on fly ash could be explained both by Langmuir and Freundlich isotherms. Because  $R^2$  values of the linearization of both Langmuir and Freundlich isotherms were the highest and almost equal. Since it is known that no one isotherm can describe all behavior over all ranges of surface coverage and concentration, our findings should be considered meaningful.

While adsorption behavior of boron on demineralized lignite could be explained mainly by Langmuir isotherm ( $R^2= 0.9953$ ), the adsorption on zeolite could be explained mainly by Freundlich isotherm ( $R^2=0.9985$ ). Values in Table 2 reveal the extent of adsorption on different adsorbents.  $C_m$  and  $L$  explained why the adsorption on fly ash was much greater compared with those of demineralized lignite and zeolite.  $L$  is the equilibrium constant

relating rates of adsorption and desorption ( $L=k_a/k_d$ ). Greater values of  $L$  indicated higher rates of adsorption rather than desorption, which suggested more material adsorbed on the adsorbent.  $L$  value for the fly ash was much greater than those of other adsorbents. This was also an indication why the extent of adsorption on fly ash was the greatest among other adsorbents.

The Freundlich isotherm represents the data at low and intermediate concentrations and is a good model for heterogeneous surfaces. When the value of Freundlich constant  $n_f$  is equal to unity, Freundlich equation becomes linear and the Freundlich constant  $K_f$  becomes equivalent to the distribution ratio, which is an empirical constant usually used in the quantification of the sorption process [48]. If the value of  $n_f$  is equal to unity, the adsorption is linear and it indicates that adsorption sites are homogeneous in energy and no interaction takes place between the adsorbed species. As implied by the values of  $n_f$ , sorption seems to be highly nonlinear for fly ash and demineralized lignite but close to unity in the case of zeolite. This indicates a fast decrease in the fixation capacity of the sorbent sites as the initial concentration is increased. Since Freundlich isotherm does not predict a maximum coverage for a given sorbent, it is hard to say that  $K_f$  corresponds to the maximum sorption capacity. The value of  $K_f$  can, however, be correlated with the sorption capacity of the sorbent under the particular experimental conditions and can be useful in providing a qualitative comparison for the fixation ability of a given sorbent towards different sorbates.

$X_m$  and  $k$  values were obtained by plotting  $\ln C_s$  versus  $\epsilon^2$  at various temperatures. The slope of line yields  $k$  ( $\text{mol}^2/\text{kJ}^2$ ) and the intercept is equal to  $\ln X_m$ . The results were presented in Table 3. The mean free energy of adsorption known as the free energy change when one mol adsorbate is transferred from infinity in solution to the surface of the adsorbent was obtained from the following relationship  $E = -(2k)^{-0.5}$  given by Hobson [41]. DR parameters were given in Table 3. As can be seen in Table 3, correlation factors ( $R^2$ ) are in the range 0.9514–0.9852 for fly ash at 25°C. The magnitude of free energy is used for estimating the type of adsorption [42].  $E$  values are in the range of 3.116–7.036 kJ/mol. Since  $E$  values found in our work are less than 8 kJ/mol, physical adsorption due to weak van der Waals forces [42,43] was also occurring in addition to chemisorptions that was observed by the Type I isotherms.  $X_m$  values increased with increasing of temperature from 25 to 45°C for fly ash.

## Adsorption Thermodynamics

Standard entropy and enthalpy changes of the adsorption of boron on fly ash were calculated as,  $\Delta S^0 = -0.690$  kJ/molK and  $\Delta H^0 = -215.34$  kJ/mol, respectively. As can be seen from Table 4,  $K_c$  values are decreasing with increase in temperature. In contrast,  $\Delta G^0$  values increased when the temperature increased. The negative values of  $\Delta G^0$  implied that the adsorption of boron on fly ash samples was spontaneous. The negative value of  $\Delta S^0$  indicated the decreased randomness at the solid/solution interface during the adsorption boron on the fly ash sample. Negative value of  $\Delta H^0$  showed the exothermic nature of the process. Negative  $\Delta S^0$  values correspond to a decrease in degree of freedom of the adsorbed species. In addition to this, since values of  $\Delta G^0$  increased with an increase in temperature, the spontaneous nature of adsorption is inversely proportional to the temperature.

## Adsorption Kinetics

Change of adsorption of boron by fly ash zeolite and demineralized lignite with time at 25°C is shown in Fig. 9. The effect of contact time on the amount of boron adsorbed onto adsorbents was examined at the optimum initial concentration of boron. As can be seen from Fig. 9, the maximum amounts of adsorption of boron onto all of adsorbents were observed at about 25 hours. There is almost no further increase of adsorption after 25 hours. Therefore it can be accepted as optimum contact time. Several kinetic models have been applied with a view to finding out the adsorption mechanism of boron onto fly ash sample since the highest adsorption of boron was observed with the fly ash [40].

First,  $1/q_t$  was plotted versus  $1/t$  to investigate the fit of pseudo-first-order-kinetics to boron adsorption. From the linear correlation analysis it is estimated that the values of the correlation coefficient ( $R^2_1$ ) for the pseudo-first-order model is 0.869, for fly ash at initial boron concentration of 10 ppm (~1 mmol/L). Coefficient for pseudo-second order kinetic ( $R^2_2$ ) was obtained by plotting  $t/q_t$  versus  $t$  and this coefficient was found to be 0.983. Third, the plot of  $q_t$  versus  $t^{1/2}$  for the intraparticle diffusion model was tested. Correlation coefficient for intraparticle diffusion ( $R^2_p$ ) value was 0.958. As conclusion it  $R^2_2$  values are greater than those of other rate laws and it might be stated that the adsorption of boron on fly ash was occurring with a pseudo-second order kinetic model. Since intraparticle diffusion model

coefficient ( $R_p^2$ ) was also relatively significant, it might also be concluded that intraparticle diffusion of the boron species had also some effect in the adsorption kinetics.

## CONCLUSIONS

- a. This study demonstrated that boron removal from aqueous solutions was controlled by the material type and operational conditions (pH, dose of the adsorbent). Boron in aqueous solutions could be removed with fly ash, zeolite and demineralized lignite with different capacities. Utilization of zeolite and demineralized coal were not that successful in removing boron from aqueous solutions. Experiments showed that a considerable amount of boron (>90%) could be removed using fly ash as the adsorbing medium. Therefore fly ash, a waste product of power stations, can be successfully used to remove boron from contaminated waters.
- b. The results indicated that boron removal by all the adsorbents were affected by the pH of the solution. It seemed that maximum adsorption was achieved in the pH range of 10-11 for all of the adsorbents. Boron removal by fly ash was strongly dependent on the pH.
- c. Adsorption of boron with the amount of adsorbent increased in all of the adsorbents. The effect was more pronounced in the case of fly ash. As the amount of the fly ash was increased from 20 g/L to 100.0 g/L the percentage of adsorbed boron increased from 47 to 94, respectively.
- d. The isotherms of boron adsorption for all adsorbents can be classified as type I isotherm. Analyses of the results obtained revealed that the adsorption of boron on fly ash could be explained both by Langmuir and Freundlich isotherms.
- e. Dubinin-Radushkevich model was used to calculate adsorption energies. Standard entropy and enthalpy changes of the adsorption of boron on fly ash were calculated as,  $\Delta S^0 = -0.69$  kJ/molK and  $\Delta H^0 = -215.34$  kJ/mol.
- f. The negative values of  $\Delta G^0$  implied that the adsorption of boron on fly ash samples was spontaneous. The negative value of  $\Delta S^0$  indicated the decreased randomness at the solid/solution interface during the adsorption boron on the fly ash sample. negative values of  $\Delta H^0$  show the exothermic nature of the process.

- g. The adsorption of boron on fly ash was occurring with a pseudo-second order kinetic model and intraparticle diffusion of the boron species had also some effect in the adsorption kinetics.

## REFERENCES

1. Lyday, P.A. (2003) Boron, Minerals Yearbook, I at URL <http://minerals.er.usgs.gov/minerals/pubs/myb.html>.
2. García-Soto, M.M.F.; Camacho, E.M. (2006) Boron removal by means of adsorption with magnesium oxide. *Sep. Purif. Technol.*, 48: 36.
3. Peak, D.; Luther, G.W.; Sparks, D.L. (2003) ATR-FTIR spectroscopic studies of boric acid adsorption on hydrous ferric oxide. *Geochim. Cosmochim. Acta*, 67: 2551.
4. Howe, P.D. (1998) A review of boron effects in the environment. *Biol. Trace Elem. Res.*, 66: 153.
5. Coughlin, J.R. (1998) Sources of human exposure: overview of water supplies as sources of boron. *Biol. Trace Elem. Res.*, 66: 87.
6. Gemici, U.; Tarcan, G. (2002) Distribution of boron in thermal waters of western Anatolia, Turkey and examples of their environmental impacts. *J. Environ. Geology*, 43: 87.
7. Demirel Z.; Yildirim, N. (2002) Boron pollution due to geothermal wastewater discharge into the Büyük Menderes river, Turkey. *Int. J Environ. Pollution*, 18: 602.
8. World Health Organization, (1993) Guidelines for Drinking Water Quality, 2nd ed. Geneva.
9. Weinthal, E.; Parag, Y.; Vengosh, A.; Muti, A.; Kloppmann, W. (2005) The EU drinking water directive: The boron standard and scientific uncertainty. *Eur. Env.*, 15: 1.
10. Mastromatteo E.; Sullivan, F. (1994) Summary: International Symposium on the Health Effects of Boron and Its Compounds. *Environ. Health Perspectives*, 102: 139.
11. Matsumoto, M.; Kondo, K.; Hirata, M.S.; Kokubu, T.; Hano, T.; Takada, T. (1997) Recovery of boric acid from wastewater by solvent extraction. *Separ. Sci. Technol.*, 32: 983.
12. Murray, F.J. (1996) Issues in boron risk assessment: pivotal study, uncertainty factors and ADIs. *J. Trace Element. Experim. Med.*, 9: 231.
13. Vengosh, A.; Heumann, K.G.; Juraske S.; Kasher, R. (1994) Boron isotope application for tracing sources of contamination in groundwater. *Envi. Sci. Technol.*, 43: 231.

14. Magara, Y.; Aizawa, T.; Kunikane, S.; Itoh, M.; Kohki, M.; Kawasaki, M.; Taut, H. (1996) The behavior of inorganic constituents and disinfection by products in reverse osmosis water desalination process. *Water Sci. Technol.*, 34: 141.
15. Magara, Y.; Tabata, A.; Kohki, M.; Kawasaki, M.; Hirose, M. (1998) Development of boron reduction system for sea water desalination. *Desalination*, 118: 25.
16. Nadav, N. (1999) Boron removal from seawater reverse osmosis permeate utilizing selective ion exchange resin. *Desalination*, 124: 131.
17. Prats, D.; Chillón-Arias, M.F.; Rodríguez-Pastor, M. (2000) Analysis of the influence of pH and pressure on the elimination of boron in reverse osmosis. *Desalination*, 128: 269.
18. Pastor, M.R.; Ruiz, A.F.; Chillón-Arias, M.F.; Rico, D.P. (2001) Influence of pH in the elimination of boron by means of reverse osmosis. *Desalination*, 140: 145.
19. Kabay, N.; Bryjak, M.; Schlosser, S.; Kitis, M.; Avlonitis, S.; Matejka, Z.; Al-Mutaz, I.; Yuksel, M. (2008) Adsorption-membrane filtration (AMF) hybrid process for boron removal from seawater: an overview. *Desalination*, 223: 38.
20. Kunin R.; E. Preuss, A. (1964) Characterization of boron specific ion exchange resin. *Indust. Eng. Chem.: Prod., Res. Develop.*, 3: 304.
21. Simonnot, M.-O.; Castel, C.; Nicola, M.; Rosin, C.; Sardin, M.; Jauffret, H. (2000) Boron removal from drinking water with a boron selective resin: is the treatment really selective? *Water Res.*, 34: 109.
22. Okay, O.; Guclu, H.; Soner, E.; Balkas, T. (1985) Boron pollution in the Simav River, Turkey and various methods of boron removal. *Water Res.*, 19: 857.
23. Recepoglu, O.; Beker, U. (1991) A preliminary study of boron removal from Kizildere Turkey geothermal waste water. *Geotechnics*, 20: 83.
24. Badruk, M.; Kabay, N.; Demircioglu, M.; Mordogan, H.; Ipekoglu, U. (1999) Removal of boron from wastewater of geothermal power plant by selective ion-exchange resin. I. Batch sorption-elution studies. *Sep. Sci. Technol.*, 34: 2553.
25. Sahin, S. (2002) A mathematical relationship for the explanation of ion Exchange for boron adsorption. *Desalination*, 143: 35.
26. Sabarudin, A.; Oshita, K.; Oshima, M.; Motomizu, S. (2005) Synthesis of cross-linked chitosan possessing N-methyl-d-glucamine moiety (CCTS-NMDG) for adsorption/concentration of boron in water samples and its accurate measurement by ICP-MS and ICP-AES. *Talanta*, 66: 136.

27. Ferreira, O.P. ; Gomes de Moraes, S.; Durán, N.; Cornejo, L.; Alves, O.L. (2006) Evaluation of boron removal from water by hydrotalcite-like compounds. *Chemosphere*, 62: 80.
28. del Mar de la Fuente García-Soto, M.; Camacho, E.M. (2006) Boron removal by means of adsorption with magnesium oxide, *Sep. Purif. Technol.*, 48: 36.
29. Turek, M.; Dydo, P.; Trojanowska, J.; Campen, A. (2007) Adsorption/co-precipitation—reverse osmosis system for boron removal, *Desalination*, 205: 192.
30. Bouguerra, W.; Mnif, A.; Hamrouni, B.; Dhahbi, M. (2008) Boron removal by adsorption onto activated alumina and by reverse osmosis. *Desalination*, 223: 31.
31. Bryjak, M.; Wolska, J.; Kabay, N. (2008) Removal of boron from seawater by adsorption—membrane hybrid process: implementation and challenges. *Desalination*, 223: 57.
32. Çengeloglu, Y.; Tor, A.; Arslan, G.; Ersoz, M.; Gezgin, S. (2007) Removal of boron from aqueous solution by using neutralized red mud. *J. Hazard. Mater.*, 142: 412.
33. Öztürk, N.; Kavak, D.; Köse, T.E. (2008) Boron removal from aqueous solution by reverse osmosis. *Desalination*, 223:1.
34. Köse, T. E.; Öztürk, N. (2008) Boron removal from aqueous solutions by ion-exchange resin: Column sorption–elution studies. *J. Hazard. Mater.*, 152: 744.
35. Kavak, D. (2009) Removal of boron from aqueous solutions by batch adsorption on calcined alunite using experimental design. *J. Hazard. Mater.*, 163: 308.
36. Polat, H.; Vengosh, A.; Pankratov, I.; Polat, M. (2004) A new methodology for removal of boron from water by coal and fly ash. *Desalination*, 164: 173.
37. Bouguerra, W.; Mnif, A.; Hamrouni, B.; Dhahbi, M. (2008) Boron removal by adsorption onto activated alumina and by reverse osmosis. *Desalination*, 223: 31.
38. Querol, X.; Whateley, M.K.G.; Fernfíndez-Turiel, J.L.; Tuncali, E. (1997) Geological controls on the mineralogy and geochemistry of the Beypazari lignite, central Anatolia, Turkey. *Int. J. Coal Geol.*, 33: 255.
39. Yürüm, Y.; Kramer, R.; Levy, M. (1985) Interaction of kerogen and mineral matrix of an oil shale in an oxidative atmosphere. *Thermochim. Acta*, 94: 285.
40. Yurdakoç, M.; Seki, Y.; Karahan, S.; Yurdakoç, K. (2005) Kinetic and thermodynamic studies of boron removal by Siral 5, Siral 40, and Siral 80. *J. Colloid Interface Sci.*, 286: 440.
41. Hobson, J.P. (1969) Physical adsorption isotherms extending from ultrahigh vacuum to vapor pressure. *J. Phys. Chem.*, 73: 2720.

42. Mahramanlioglu, M.; Kizilcikli, I.; Bicer, I.O. (2002) Adsorption of fluoride from aqueous solution by acid treated spent bleaching earth. *J. Fluorine Chem.*, 115: 41.
43. Singh, T.S.; Pant, K.K. (2004) Equilibrium, kinetics and thermodynamic studies for adsorption of As (III) on activated alumina. *Sep. Purif. Technol.*, 36: 139.
44. Kannan, N.; Sundaram, M.M. (2001) Kinetics and mechanism of removal of methylene blue by adsorption on various carbons—a comparative study. *Dye. Pigment.*, 51: 25.
45. Ho, Y.S.; Wase, D.A.J.; Forster, C.F. (1996) Kinetic Studies of Competitive Heavy Metal Adsorption by Sphagnum Moss Peat. *Environ. Technol.*, 17: 71.
46. Weber Jr., W.J.; Morriss, J.C. (1963) Kinetics of adsorption on carbon from solution. *J. Sanitary Eng. Div. Am. Soc. Civ. Eng.*, 89: 31.
47. Yürüm, Y.; Dror, Y.; Levy, M. (1985) Effects of acid dissolution on the organic matrix of the Zefa Efe oil shale. *Fuel Process. Technol.*, 11: 71.
48. Shahwan, T.; Erten, H.N. (1999) Radiochemical Study of  $\text{Co}^{2+}$  Sorption on Chlorite and Kaolinite. *J. Radioanal. Nucl. Chem.*, 241: 151.

**Table 1.** Chemical analyses of the demineralized lignite, zeolite and fly ash samples and surface characteristics.

<b>Elemental Analysis of Bey pazari Lignite, (dry and mineral matter free basis) % by weight</b>		<b>Chemical Group</b>	<b>Zeolite, % (by weight)</b>	<b>Fly Ash, % (by weight)</b>
		<b>SiO<sub>2</sub></b>	71.0	16.8
		<b>CaO</b>	3.4	44.2
		<b>Fe<sub>2</sub>O<sub>3</sub></b>	1.7	3.8
		<b>Al<sub>2</sub>O<sub>3</sub></b>	11.8	9.1
<b>C</b>	61.2	<b>K<sub>2</sub>O</b>	2.4	1.4
<b>H</b>	5.5	<b>MgO</b>	1.4	2.3
<b>N</b>	1.9	<b>Na<sub>2</sub>O</b>	0.4	2.7
<b>S (Total)</b>	5.3	<b>TiO<sub>2</sub></b>	0.1	0.5
<b>O (by difference)</b>	26.1	<b>P<sub>2</sub>O<sub>5</sub></b>	-	0.2
<b>B<sub>2</sub>O<sub>3</sub> (with ICP)</b>	-	<b>B<sub>2</sub>O<sub>3</sub> (with ICP)</b>	-	-
<b>Surface Characteristics of the Adsorbents</b>				
<b>Adsorbent</b>		<b>Surface Area, m<sup>2</sup>/g</b>	<b>Pore Volume, cm<sup>3</sup>/g</b>	<b>Pore Radius, nm</b>
Fly Ash		7.2	0.19	57.5
Zeolite		10.2	0.11	22.1
Demineralized Lignite		31.1	0.08	23.7

**Table 2.** Langmuir, Freundlich and Dubinin Radushkevich isotherm constants for different sorbents at 25°C.

Sorbent	Langmuir Constants			Freundlich Constants			Dubinin-Radushkevich Constants		
	R <sup>2</sup>	C <sub>m</sub> , mmol/g	ℒ L/mmol	R <sup>2</sup>	K <sub>f</sub> , mmol/g	n <sub>f</sub>	R <sup>2</sup>	X <sub>m</sub> , mol/g	k, mol <sup>2</sup> /kJ <sup>2</sup>
Demineralized lignite	0.9953	0.0076	2.172	0.9868	0.0051	0.338	0.9593	0.0063	0.0622
Zeolite	0.9792	0.0031	0.365	0.9985	0.0008	0.7711	0.9380	0.0012	0.1082
Fly ash	0.9969	0.0275	24.52	0.9973	0.0334	0.2452	0.9852	0.0273	0.0101

**Table 3.** Dubinin-Radushkevich constants and adsorption energies for fly ash at different temperatures.

<b>T, °C</b>	<b>R<sup>2</sup></b>	<b>X<sub>m</sub>, mol/g</b>	<b>k, mol<sup>2</sup>/kJ<sup>2</sup></b>	<b>-E, kJ/mol</b>
25	0.9852	0.0273	0.0101	7.036
35	0.9838	0.8699	0.0297	4.103
45	0.9514	0.2758	0.0515	3.116

**Table 4.** Equilibrium constants and standard Gibb's free energy changes for fly ash at three different temperatures and standard enthalpy change of adsorption and standard entropy change of adsorption for fly ash.

<b><math>T</math>, K</b>	<b><math>K_c</math>, L/g</b>	<b><math>\Delta G^0</math>, kJ/mol</b>	<b><math>\Delta H^0_{ads}</math>, kJ/mol</b>	<b><math>\Delta S^0_{ads}</math>, kJ/mol K</b>
298	52.13	-9.796	-215.34	-0.69
308	2.44	-2.282		
318	0.22	3.985		

**Table 5.** Kinetic parameters for adsorption of boron on fly ash.

<b><math>k_1</math></b> <b>(<math>h^{-1}</math>)</b>	<b><math>q_1</math></b> <b>(mg/g)</b>	<b><math>R^2_1</math></b>	<b><math>k_2</math></b> <b>(g/mg h)</b>	<b><math>q_2</math></b> <b>(mg/g)</b>	<b><math>R^2_2</math></b>	<b><math>k_p</math></b> <b>(mg/g <math>h^{1/2}</math>)</b>	<b>C</b> <b>(mg/g)</b>	<b><math>R^2_p</math></b>
2.922	0.0025	0.869	8.5158	0.0271	0.983	0.0028	0.0095	0.958

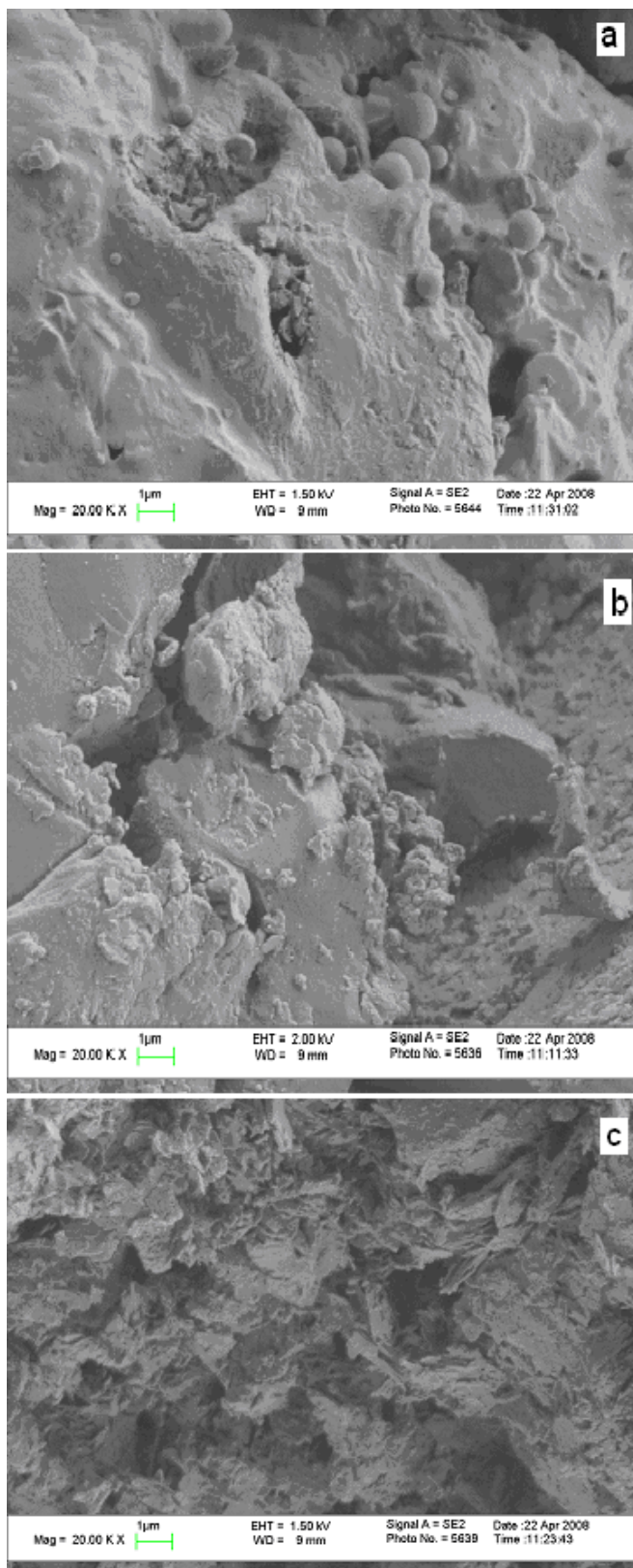


**Figure 1.** SEM images of a) fly ash, b) demineralized lignite and c) zeolite.

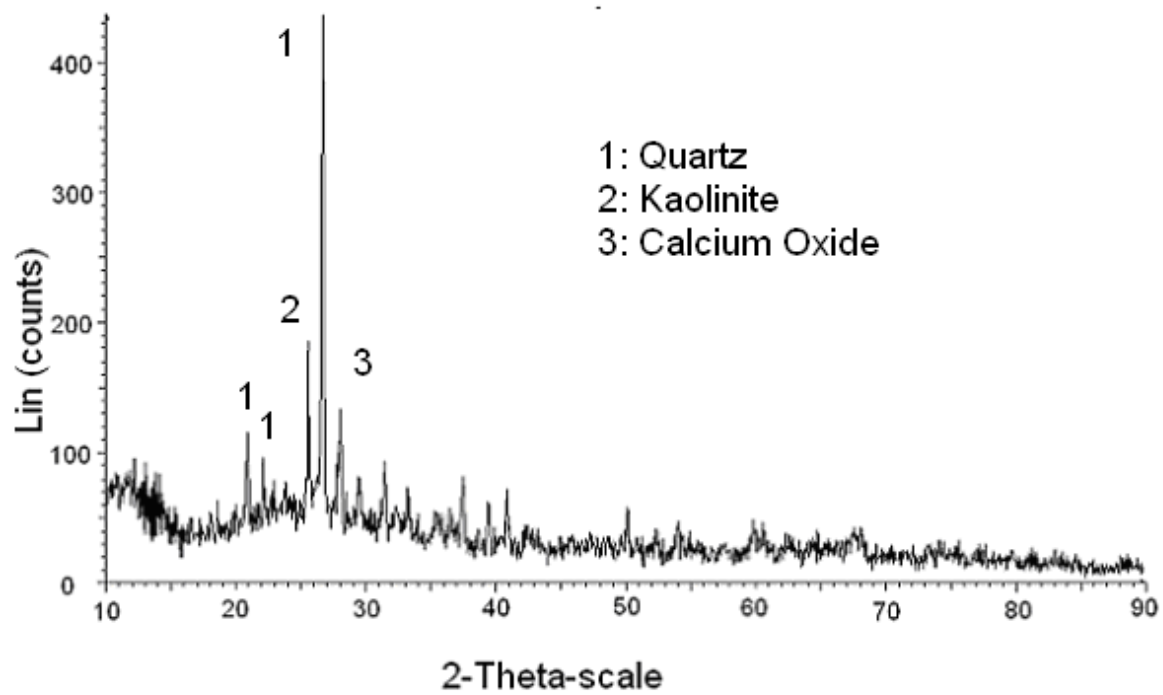


*Figure 2.* X-ray diffractogram of fly ash.

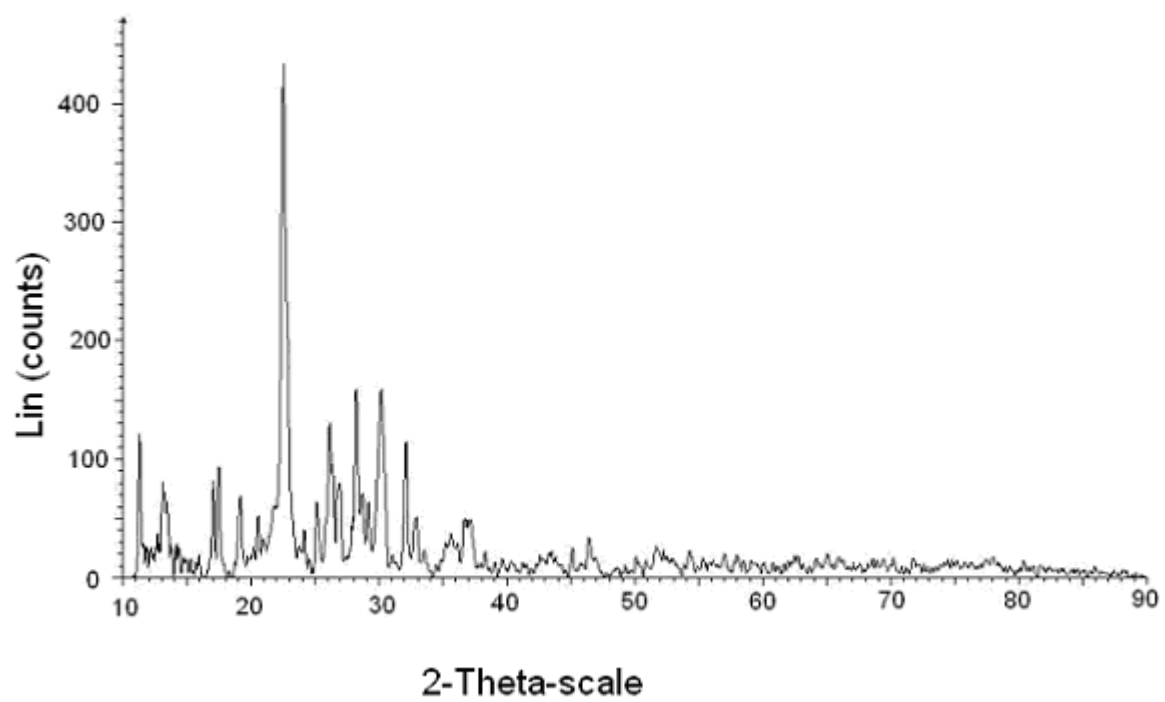


*Figure 3.* X-ray diffractogram of zeolite.

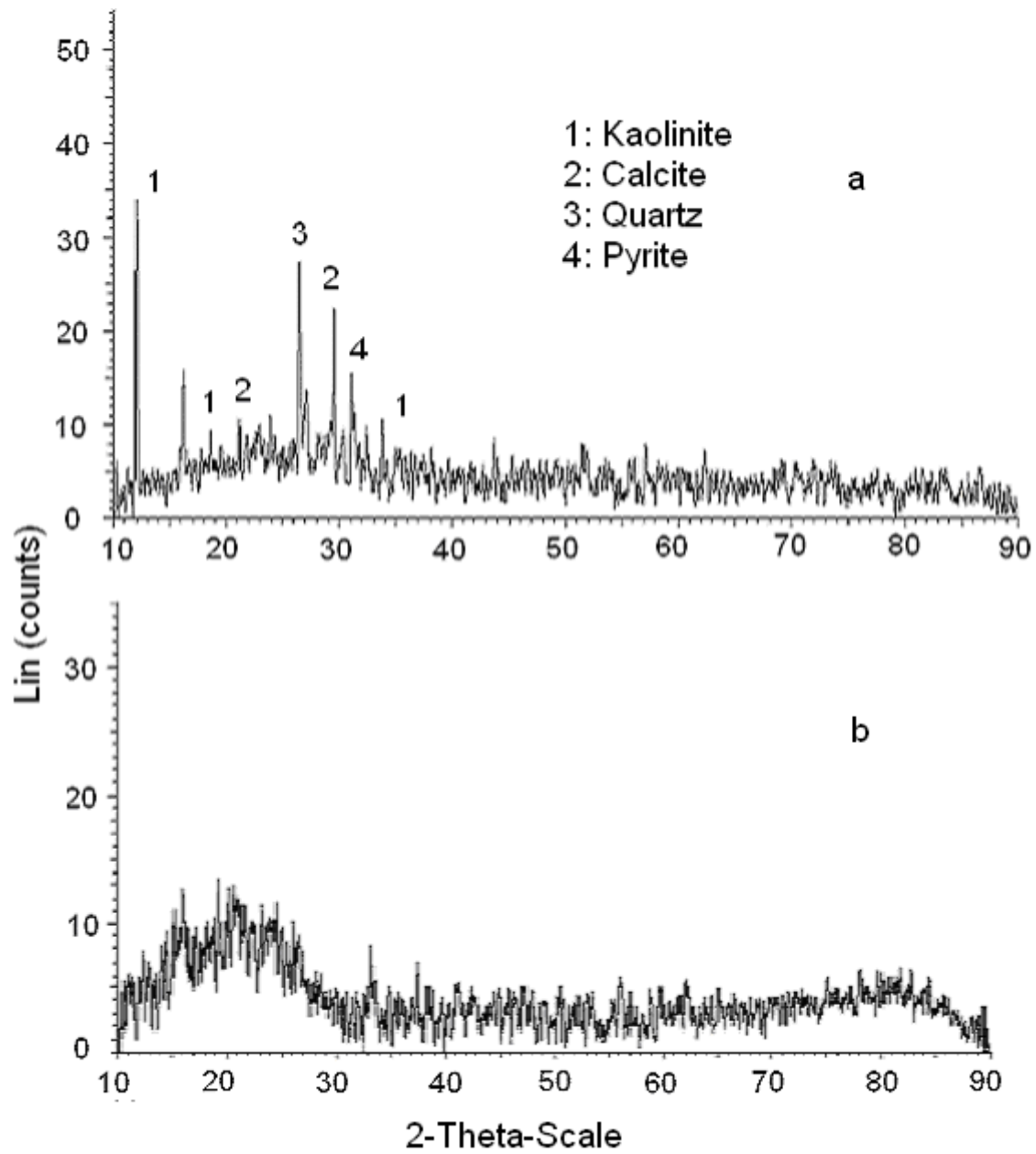


**Figure 4.** XRD results of lignite a) before and b) after demineralization.

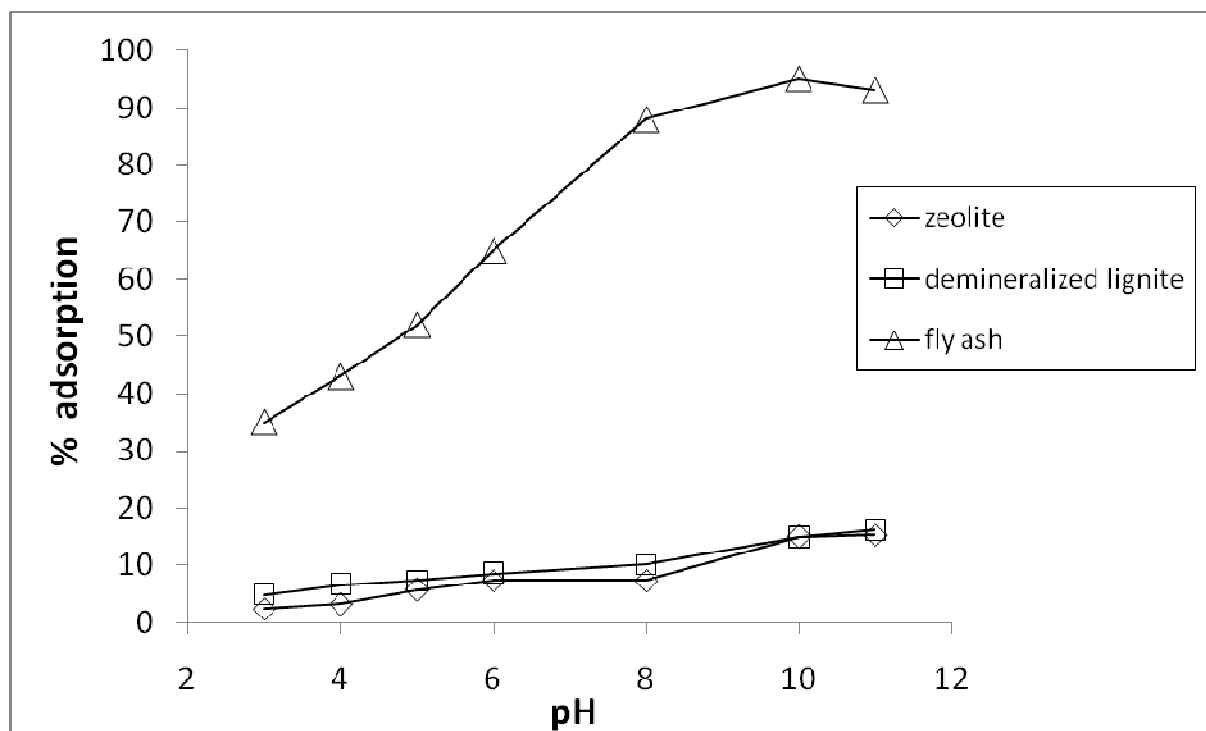


**Figure 5.** Percent adsorption as a function of pH for fly ash, demineralized lignite and zeolite, (T = 25°C, adsorbent concentration = 40 g/L, initial B concentration = 10 ppm (~1 mmol/L), adsorption time = 24 hours).

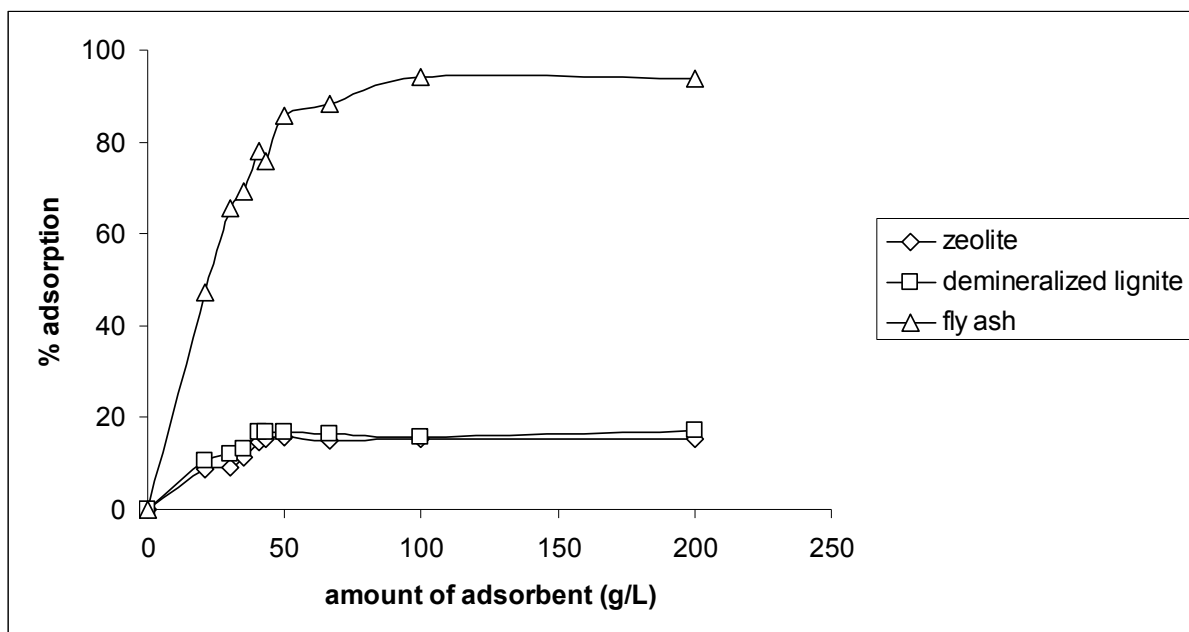


**Figure 6.** Percent adsorption as a function of adsorbent concentration (g/L) for zeolite, demineralized lignite and fly ash ( $T = 25^{\circ}\text{C}$ ,  $\text{pH} = 10$ , initial B concentration = 10 ppm ( $\sim 1$  mmol/L), adsorption time = 24 hours).

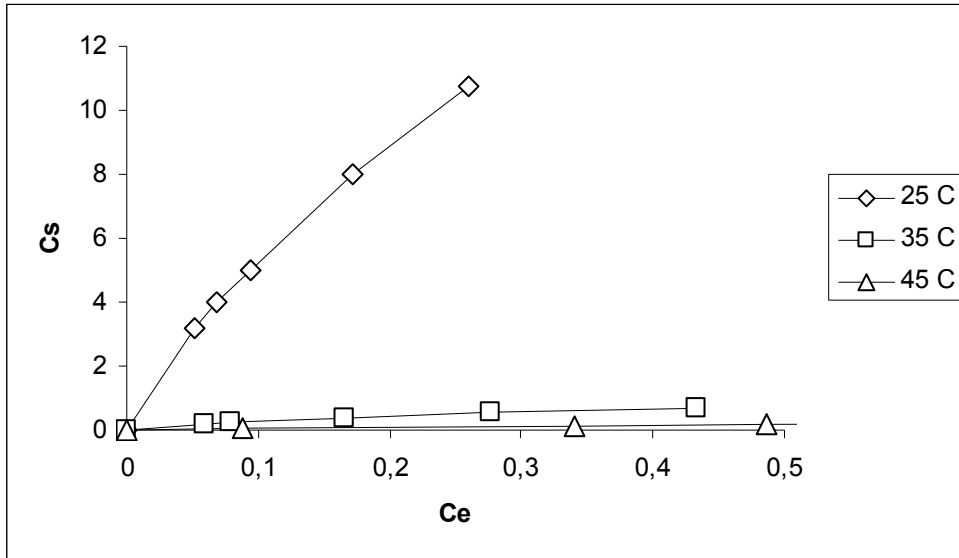


**Figure 7.**  $C_s$  (mmol/g) vs  $C_e$  (mmol/L) for fly ash at different temperatures.

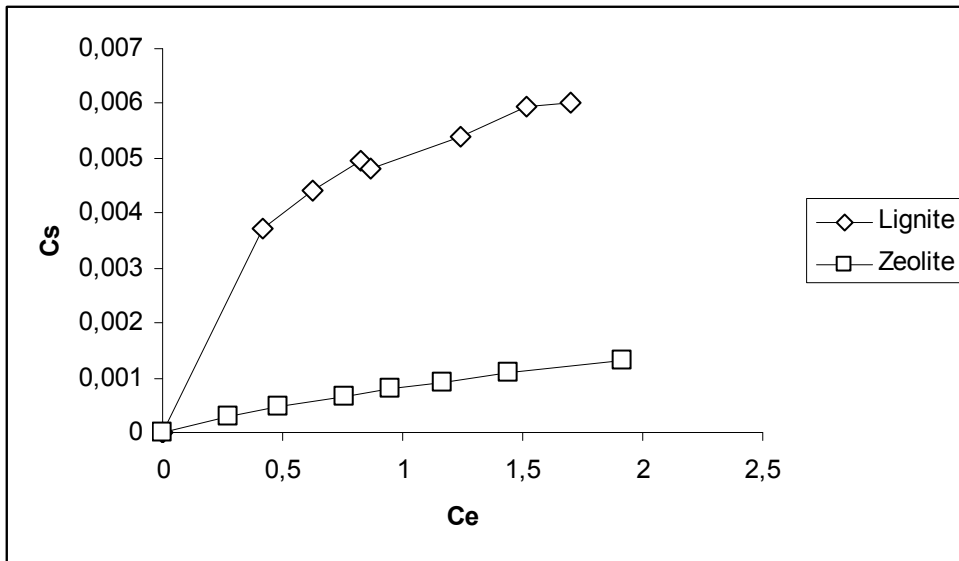


**Figure 8.**  $C_s$  (mmol/g) vs  $C_e$  (mmol/L) for demineralized lignite and zeolite at 25°C.

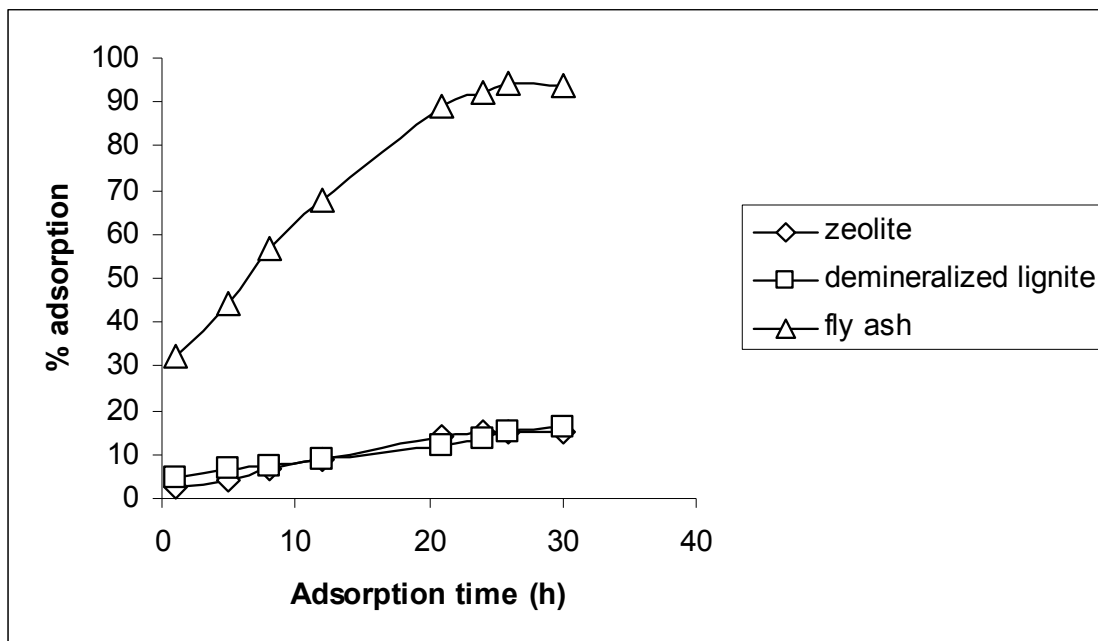


**Figure 9.** Adsorbed boron mass as a function of time (h) for zeolite (clinoptilolite), demineralized lignite and fly ash ( $T = 25^{\circ}\text{C}$ ,  $\text{pH} = 10$ , adsorbent concentration = 40 g/l, initial B concentration = 10 ppm ( $\sim 1 \text{ mmol/L}$ )).

## List of Tables

**Table 1.** Chemical analyses of the demineralized lignite, zeolite and fly ash samples and surface characteristics.

**Table 2.** Langmuir, Freundlich and Dubinin Radushkevich isotherm constants for different sorbents at 25°C.

**Table 3.** Dubinin-Radushkevich constants and adsorption energies for fly ash at different temperatures.

**Table 4.** Equilibrium constants and standard Gibb's free energy changes for fly ash at three different temperatures and standard enthalpy change of adsorption and standard entropy change of adsorption for fly ash.

**Table 5.** Kinetic parameters for adsorption of boron on fly ash.

## Figure Legends

**Figure 1.** SEM images of a) fly ash, b) demineralized lignite and c) zeolite.

**Figure 2.** X-ray diffractogram of fly ash.

**Figure 3.** X-ray diffractogram of zeolite.

**Figure 4.** XRD results of lignite a) before and b) after demineralization.

**Figure 5.** Percent adsorption as a function of pH for fly ash, demineralized lignite and zeolite, (T = 25°C, adsorbent concentration = 40 g/L, initial B concentration = 10 ppm (~1 mmol/L), adsorption time = 24 hours).

**Figure 6.** Percent adsorption as a function of adsorbent concentration (g/L) for zeolite, demineralized lignite and fly ash (T = 25°C, pH = 10, initial B concentration = 10 ppm (~1 mmol/L), adsorption time = 24 hours).

**Figure 7.**  $C_s$  (mmol/g) vs  $C_e$  (mmol/L) for fly ash at different temperatures.

**Figure 8.**  $C_s$  (mmol/g) vs  $C_e$  (mmol/L) for demineralized lignite and zeolite at 25°C.

**Figure 9.** Adsorbed boron mass as a function of time (h) for zeolite (clinoptilolite), demineralized lignite and fly ash (T = 25°C, pH = 10, adsorbent concentration = 40 g/L, initial B concentration = 10 ppm (~1 mmol/L)).